Analysis of groundwater migration from artificial recharge in a large urban aquifer: A simulation perspective

Andrew F. B. Tompson, Steven F. Carle, Nina D. Rosenberg,
and Reed M. Maxwell
Geosciences and Environmental Technologies Division,
Lawrence Livermore National Laboratory, Livermore, CA 94551

September 10, 1998

Abstract

The increased use of reclaimed water for artifical groundwater recharge purposes has led to concerns about future groundwater quality, particularly as it relates to the introduction of new organic and inorganic contaminants into the subsurface. Here, we review the development and initial application of a detailed numerical model of groundwater flow and migration in a region encompassing a large groundwater recharge operation in Orange County, California. The model is based upon a novel representation of geologic heterogeneity, which has long been known to influence local flow and transport behavior in the subsurface. The model – and complementary series of isotopic analyses – provide an improved scientific basis to understand flow paths, migration rates, and residence times of recharged groundwater, as well as to identify the source composition of water produced in wells near the recharge operation. From a management perspective, these issues need to be confronted in order to respond to proposed regulatory constraints that would govern the operation of recharge facilities and nearby production wells. While model calibration is greatly aided by isotopic source and residence time analyses, the model also provides unique insights on the interpretation of isotopic data themselves. Isotopic estimates of groundwater age help discriminate between several equally-acceptable simulations calibrated to head data only. However, the results also suggest that groundwater reaching a well spans a wide ranging distribution of age, demonstrating the importance of geologic heterogeneity in affecting flow paths, mixing, and residence times in the vicinity of recharge basins and wells.

1 Background

Groundwater is a significant source of drinking water in the US and rest of the world. In California alone, groundwater supplies 40% of the agricultural and urban water demand, despite the fact that the state relies heavily on surface water provided by numerous reservoir and aqueduct systems. As a result of urban growth, mandated environmental uses, uncertainties produced by drought, and limited opportunities for expansion of the existing reservoir system, many water districts are considering the acquisition of new or additional sources of groundwater to meet growing and disparate water demands.

Increased reliance on groundwater necessitates improved aquifer management with respect to understanding large recharge and discharge issues, planning rates of withdrawal, balancing demands of multiple users, and dealing with water quality problems arising from industrial and agricultural contamination, artificial recharge, and salt water intrusion. In California and elsewhere, artificial recharge practices are increasingly being used as a means to augment groundwater availability and improve the overall reliability of water supplies.

In this paper, we are concerned with the fate of artificial recharge in the large urban aquifer system underlying Orange County, California, especially in terms of its long term water quality implications. We will explore the use of a detailed geologic model of the aquifer system and numerical simulation as a basis to gain new scientific insight into these issues. We will also discuss how this approach has benefited from and contributed to similar efforts conducted from an isotopic analysis perspective.

1.1 The Orange County groundwater system

The Orange County Water District (OCWD) manages a groundwater basin that provides 70% of the domestic water supply for approximately 2 million residents in the northern part of Orange County, California (OCWD, 1991, 1995). The remaining 30% is purchased and imported from outside the district. On an average annual basis, roughly 270,000 acre feet (af) of water are extracted from several hundred production wells located within the middle production aquifers of the basin. These units can be over 1,000 ft thick, and generally extend the entire width of the basin, from the "Forebay" area (under mostly phreatic conditions) toward the confined "Pressure Zone" that abuts the Pacific Ocean and Newport-Inglewood Fault (Figs. 1 and 2).

To sustain this rate of withdrawal, OCWD maintains an active recharge effort that returns about 205,000 af of water, on an annual basis, to the groundwater basin. This is achieved by diverting large portions of the base flow of the Santa Ana River and additional imported water into a series of infiltration basins and abandoned gravel pits in the Forebay along or nearby the upper reaches of the river (Figs. 1 and 3). Water recharged in the Forebay can easily be drawn into the middle aquifers (Fig. 2), as well as a shallow aquifer in the Pressure Zone and a

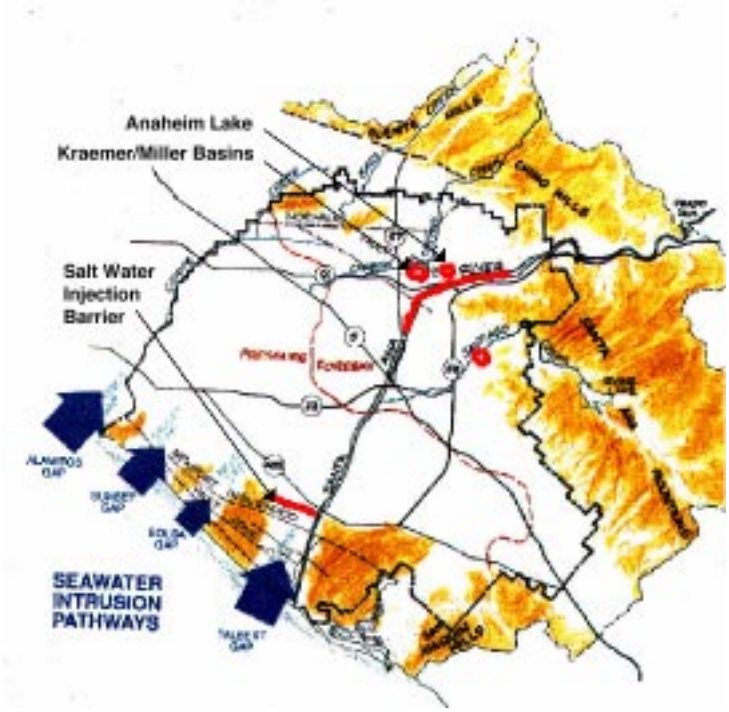

Figure 1: Plan view of the Orange County Water District boundaries (dashed line) showing sea water intrusion pathways, Forebay recharge areas, and the salt water barrier injection area. The Santa Ana River runs directly through the district for a length of approximately 20 miles (from OCWD, 1991)

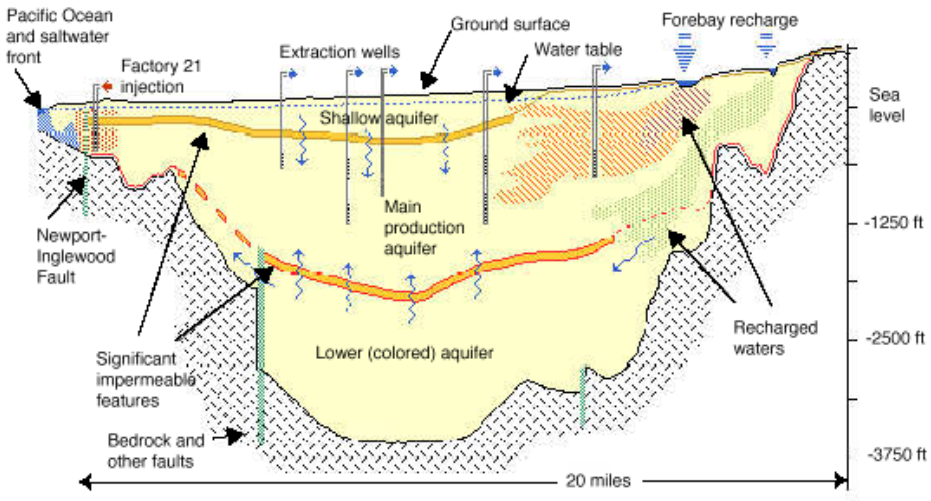

Figure 2: Vertical cross-section of the Orange County groundwater basin, approximately paralleling the Santa Ana River, with the Pacific Ocean to the left. Water recharged in the "Forebay" area (right) can migrate in a westerly direction into the main (middle) production aquifer, as well as the shallow and lower aquifers.

much deeper colored water aquifer that is not used for production (OCWD, 1991). In the future, planners are considering increasing the Forebay recharge to support close to 100% of the water demand from groundwater (OCWD, 1991).

Near the Pacific coast, OCWD also reinjects between 5,000 and 10,000 af of reclaimed water from their Factory 21 treatment plant into the shallow aquifer to form a saltwater intrusion barrier. This serves to prevent further salt water migration into the middle production aquifers beneath a break in the confining unit (Fig. 2). Because of the faulted structures along the coast, much of the basin is generally protected from significant salt water intrusion.

1.2 Use of reclaimed water

The principal source of water for current Forebay recharge operations is derived from the surfacewater flows in the Santa Ana River. Recharge in the Forebay is occasionally supplemented with water imported from the Colorado River and other State Water Project sources. Future plans call for using reclaimed water from the Factory 21 treatment plant as a means to increase the overall recharge in the Forebay area. Interestingly, much of the base flow in the Santa Ana River today is itself "reclaimed" because it is largely comprised of discharges from upstream treatment plants in Riverside County. Use of recycled or reclaimed water for recharge or other secondary use purposes is becoming more widespread throughout the world. There are numerous water quality issues are associated with these practices.

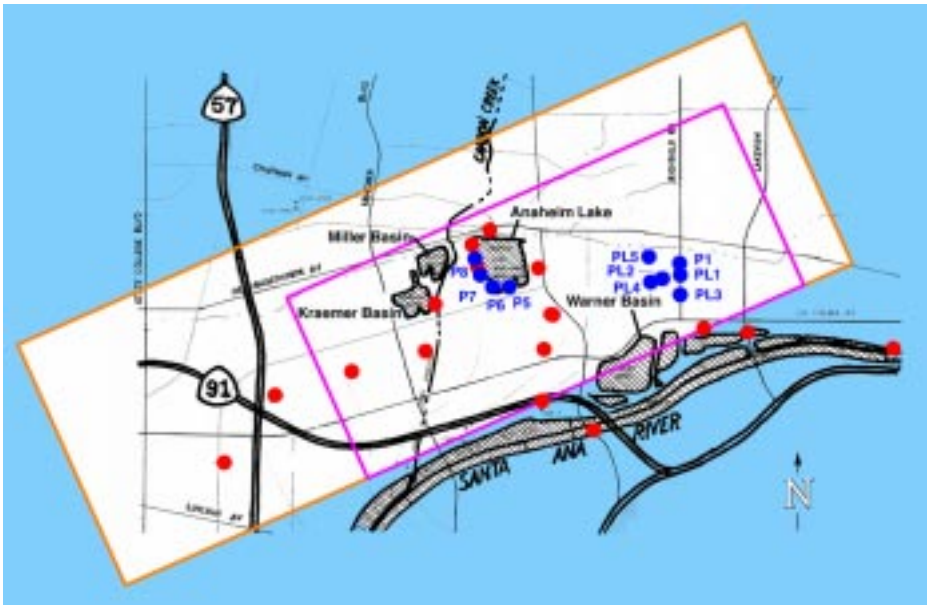

Figure 3: Plan view of the Forebay area showing the Santa Ana River and principal recharge basins. The larger outlined box indicates the top portion of the original 3D geologic model domain. The smaller box corresponds to the top of the actual flow model domain. Labeled dots represent the 10 production wells used in the flow model, 6 of which were used for geologic characterization purposes. Unlabeled dots represent 18 additional monitoring wells used in the characterization process.

1.3 Water quality implications

In a recharge or reinjection scenario, reclaimed wastewater may introduce organic or microbiological contaminants into groundwater that may later be captured in production wells. In the absence of advanced treatment methods, a continual process of recycling may also tend to increase the inorganic salt (or total dissolved solid, TDS) loading in waters, over and above agricultural inputs and other background sources.

Because dilution, natural degradation and other transformation processes may serve to lower contaminant concentrations along travel pathways, state regulators in California have proposed a nominal series of standards to govern how production wells and recharge practices involving reclaimed water are operated. These standards complement existing standards for TDS and other contaminants in drinking water, and would require that

- All reclaimed water returned to an aquifer have a specified residence time before reaching production wells, as a way to ensure that degradation or dilution mechanisms occur;
- Only a specified fraction of production well water may be reclaimed in origin, regardless of residence time; and
- Production wells be located "sufficiently far" from recharge basins or recharge wells.

For water recharged through percolation basins in the Forebay, the proposed regulations stipulate a minimum groundwater residence time of one year, a production well reclamation fraction of 50%, and a minimum distance separating production wells from the basins of 2,000 ft. Because these regulations are tentative, additional scientific study may be needed for their refinement.

1.4 Resource management challenges

As a result, OCWD has developed an interest in identifying degradation and related transformation mechanisms associated with groundwater contaminants derived from recycled sources, as well as implementing advanced and more thorough treatment methods and technologies for reclaimed water. In addition, isotopic analyses are now being used to infer historical migration patterns by estimating the composition, sources, and ages of groundwater sampled in production and monitoring wells near the spreading basins.

Below, we will review some of the isotopic results and present a series of numerical simulations designed to examine residence times, historical or future migration pathways, and mixing and dilution processes in the system. Both approaches provide different, and occasionally overlapping perspectives on system behavior.

2 Isotopic analyses

Figure 4 shows an expanded vertical cross section through the Forebay along an east-west line passing through the Santa Ana River, Anaheim Lake, and Miller/Kraemer recharge basins. Several production and monitoring wells close to the section are indicated. The geologic structure was inferred by OCWD geologists from multiple borehole analyses. The principal aquifer materials include permeable sands, sandstones, gravels, and conglomerates (white) of the surficial alluvium and the La Habra and San Pedro formations and semipermeable interbedded silts, siltstones, and clays (dark lenticular zones). At the bottom lies a relatively impermeable Tertiary basement (lower cross-hatched area).

2.1 Age dating

A series of isotopic analyses have been used to estimate the composition and ages of groundwater in wells near the spreading basins (Davisson, *et al.*, 1996, 1998). Figure 4 shows the apparent ages of ground water sampled in wells, as determined from measured tritium–helium ratios. As tritium radioactively decays to helium-3, their molar ratio ($^3H/^3He$) in groundwater becomes a barometer of residence time, regardless of the initial tritium loading (Schlosser, 1992; see Appendix). Similar studies have also been carried out near the coastal salt water barrier (Hudson, *et al.*, 1995).

The $^3H/^3He$ data clearly indicates that older water is found at greater depths. Two of the deeper "Anaheim" wells immediately adjacent to Anaheim Lake (shown as one well in Fig. 4) have apparent ages of 12 and 18 y, respectively, suggesting that the well water would easily meet a one-year residence time requirement. In shallower zones, a range of ages is found. An apparent age of 10 years measured at one of the Yorba Linda wells seems to suggest slower flow rates, possibly consistent with a greater abundance of low permeability materials in the shallow alluvium near the Santa Ana River. Very young (< 1 yr old) waters found beneath and to the west of Anaheim Lake suggest the opposite, namely, that recharge spreads rapidly into downgradient locations in the aquifer. This is consistent with an abundance of gravely materials in the alluvium and hydraulic conductivities in the range of 200 to 1,000 ft/day.

It is important to recognize that age data are reflective of the sampling size and can be affected by mixing and dispersive processes (Nir, 1964; Schlosser, 1992). Water collected in the deeper "Anaheim" wells are representative mixtures taken from 680 to 750 ft long screened intervals, which suggests that the samples surely contain waters of many different ages and sources. It is pertinent to note that $^3H/^3He$ ages determined from such mixtures are averaged, and they may differ from a separate mean of individual water ages in each vertical element of the wells. This distinction is reviewed more carefully in the Appendix.

From these perspectives, it is not clear whether all "elements" of the water sample meet the nominal one-year residence time requirement, nor is it clear how

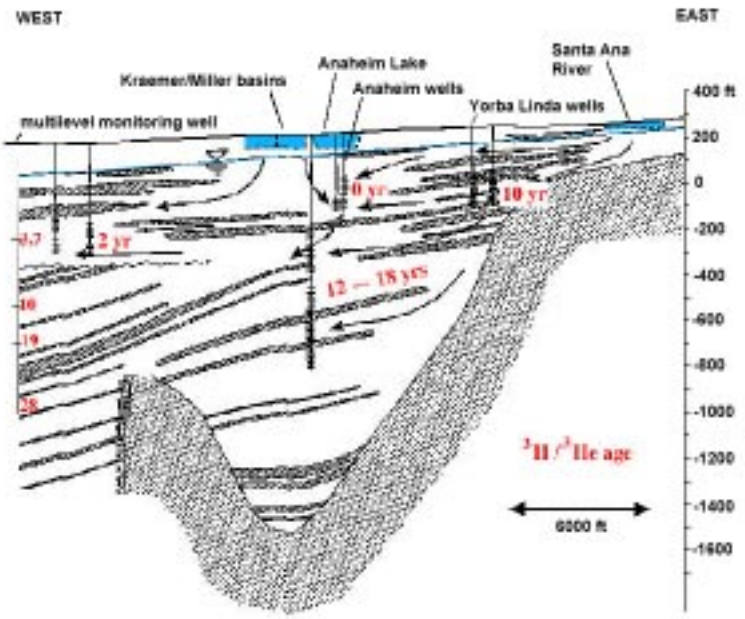

Figure 4: Expanded vertical cross section through the Forebay area along a E-W line passing through the Santa Ana River, Anaheim Lake, and Miller/Kraemer recharge basins (similar to the upper right part of Fig. 2). Numbers indicate approximate groundwater ages determined from $^3H/^3He$ ratios measured in production or monitoring wells. Arrows indicate inferred groundwater flow paths. Geologic structure inferred by OCWD geologists from multiple borehole analyses (see text). Vertical scale in feet above sea level.

or whether such requirements need to be rethought in light of the sample origin and broader mixing and dispersion issues associated with the sampling scale.

Note that water taken from the multilevel well on the left side of Figure 4 is based upon several very small monitoring ports and shows a distinct variation of age with depth.

2.2 Source, pathline, and dilution measurement

Imported water from the Colorado River water is used throughout Southern California and is frequently used to recharge Anaheim Lake. Compared with local precipitation, the Colorado River water is markedly depleted in the δ^{18}O isotope and has a distinct oxygen isotope ratio (δ^{18}O) that can be easily identified in local groundwater regimes (Williams and Rodoni, 1997). Analyses of the δ^{18}O ratio have been used to assess the fate and dilution of water released in Anaheim Lake by distinguishing the presence and concentration of Colorado River water in downgradient wells (Davisson, *et al.*, 1996, 1998). Under some conditions, noble gas analyses can also be used to distinguish groundwater that has been artificially recharged quickly through the basins, as well as infer the temperature of groundwater at the time of its recharge (Davisson, *et al.*, 1996).

3 Two-dimensional scoping model

A two dimensional model of steady groundwater flow was developed to gain insights into the processes affecting the residence times and migration pathways reflected by the isotopic data in Figure 4. The modeling approach will be used to illustrate the sensitivity of groundwater age and source distributions to geologic heterogeneity and motivate the need for a comparable three-dimensional model. In this example, simulations were constructed to focus chiefly on the water captured by the deep "Anaheim" production wells shown in the figure.

3.1 Model approach

The cross-section of Figure 4 was used as the modeling domain under the assumption that the plane of the figure is generally parallel with flow pathways in the area. The domain is approximately 28,000 ft (5.3 mi) long. The saturated zone on the western edge is roughly 1,900 ft thick. The interpreted geologic structure shown in Figure 4 was maintained to produce a relatively high-resolution simulation. Scalar (isotropic) values of hydraulic conductivity were assigned to the permeable and semipermeable materials and adjusted for experimental and calibration purposes. A fixed conductivity of 0.001 ft/day was assigned to the Tertiary basement materials.

Simulations were based upon a standard, 5-point-stencil finite difference model of steady state groundwater flow (e.g., Celia and Gray, 1992). As an approximation, flow results were determined with fixed boundary conditions, even though conditions in the real system fluctuate according to transient recharge and pumping conditions. Along the left (west) side of the domain, the head was fixed at a hydrostatic value of 50 ft above sea level. Along the right (east) side, no-flow conditions were applied to mimic a hydraulic divide or pinch-out effect. No flow conditions were used on the bottom boundary. To approximate the water table condition on the top, the existing water table was used as a fixed, specified-flux boundary, and the model was calibrated until the head at the upper right boundary approached the observed value of 250-270 ft. above sea level. A discretization of 48 ft in the horizontal and 4.8 ft in the vertical was used, resulting in a problem with over 230,000 nodes.

Steady rainfall recharge on the top of the domain was set to a steady value of 0.00027 ft/day (0.1 ft/y). Recharge from the Kraemer/Miller basins, Anaheim Lake, and Santa Ana River were estimated by dividing the mean daily influx (determined from the annual basin recharge data) by their approximate length perpendicular to the model plane. A single pumping well screened over 3 segments in a 600 ft interval was used to approximate the deepest "Anaheim" well shown in Figure 4. The pumping rate specified was based upon a typical production value of the well, albeit reduced to account for the fact that the model domain intercepts only a fraction of the well's upgradient capture zone width. The specified flux was evenly distributed over the well screen interval. No other wells were used in this model.

Groundwater ages were estimated using a Lagrangian streamline model, as opposed to solving a separate balance equation for the age, as was recently proposed by

Goode (1996). Flow results were used to develop streamlines (*e.g.,* , Schafer-Perini *et al.*, 1991) along which material "parcels" of water are moved. Under steady flow conditions, the age or residence time of a parcel of water at a specified point in the aquifer is found by integrating the time it takes for the parcel to move upstream (backwards) along the streamline passing through it to an external recharge boundary. The distribution of water residence times measured at points along the "Anaheim" well and their subsequent reinterpretation (Appendix) were used for comparisons with the field observations.

3.2 Results

The simulation results shown in Figures 5a-5c correspond to use of different hydraulic conductivity values in the permeable and semipermeable materials. The principal values used in the permeable material ranged from 150 to 300 ft/day and were generally consistent in magnitude with pump test data and calibrated values used in an 2D areal OCWD regional model (OCWD, personal communication). Nevertheless, larger values close to or above 1,000 ft/day have been inferred from the shallow isotopic studies referred to above. Conductivity values in the semi-permeable materials ranged from 0.1 to 1 ft/day, although in one case, the semipermeable zones were considered to have the same conductivity as the permeable materials (150 ft/day).

The cross-sectional images in Figures 5a-5c show contours of hydraulic head and backward travel pathways from the Anaheim well to surface recharge points. The backward trajectories were initiated on each side of the 2D well and were chosen such that each corresponded to identical fractions of the total well flux. The travel pathways are color-coded to represent travel time along each backward trajectory.

The total travel time along streamlines connecting the well to surface recharge points is shown again in the top figure. Because each trajectory corresponds to the same flux, the spatial density of points along the surface is proportional to the surface flux distribution. Shaded areas represent the integrated fraction of surface flux entering respective portions of the well from Anaheim Lake, rainfall recharge, and the Santa Ana River, respectively.

The bottom figure represents the fractional age distribution of water entering the well.

3.3 Observations

In Figure 5a, the hydraulic head distribution is clearly affected by the semipermeable materials (K =1 ft/day), as are the streamlines connecting the well to the surface. Streamlines leaving the river are tightly bunched above the abundant low permeability zones until they reach a natural break east of the lake. Water in the upper part of the well is clearly younger and dominated by lake recharge. Water in the lower part of the well is older and originates from the river and rainfall recharge in between. Altogether, 77% of the well water derives from the lake, 20% from the

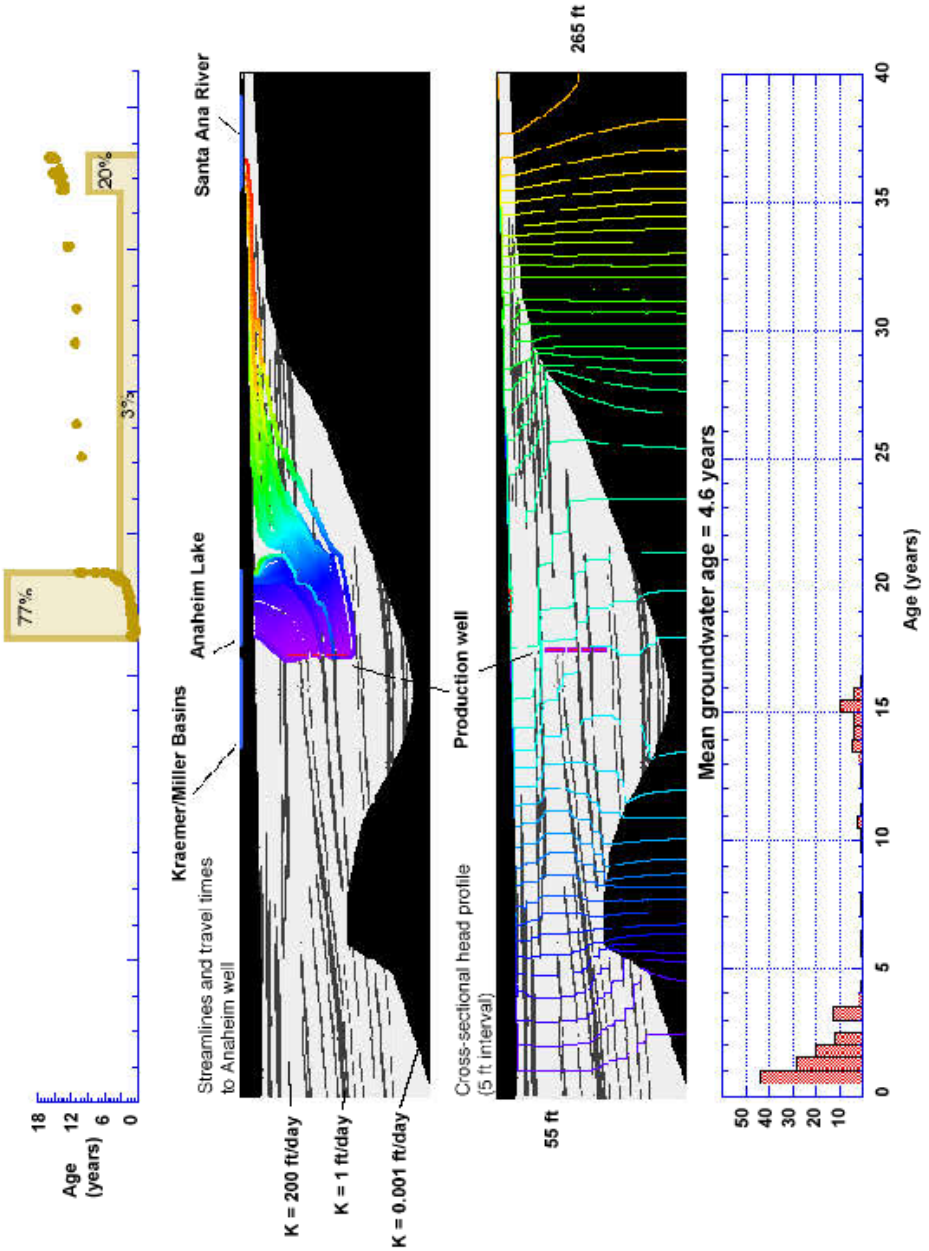
77%
20%
3%
Age (years)
18
12
6
0
Santa Ana River
Anaheim Lake
Kraemer/Miller Basins
Streamlines and travel times to Anaheim well
K = 200 ft/day
K = 1 ft/day
K = 0.001 ft/day
Production well
Cross-sectional head profile (5 ft interval)
265 ft
55 ft
Mean groundwater age = 4.6 years
50
40
30
20
10
0
5
10
15
20
25
30
35
40
Age (years)

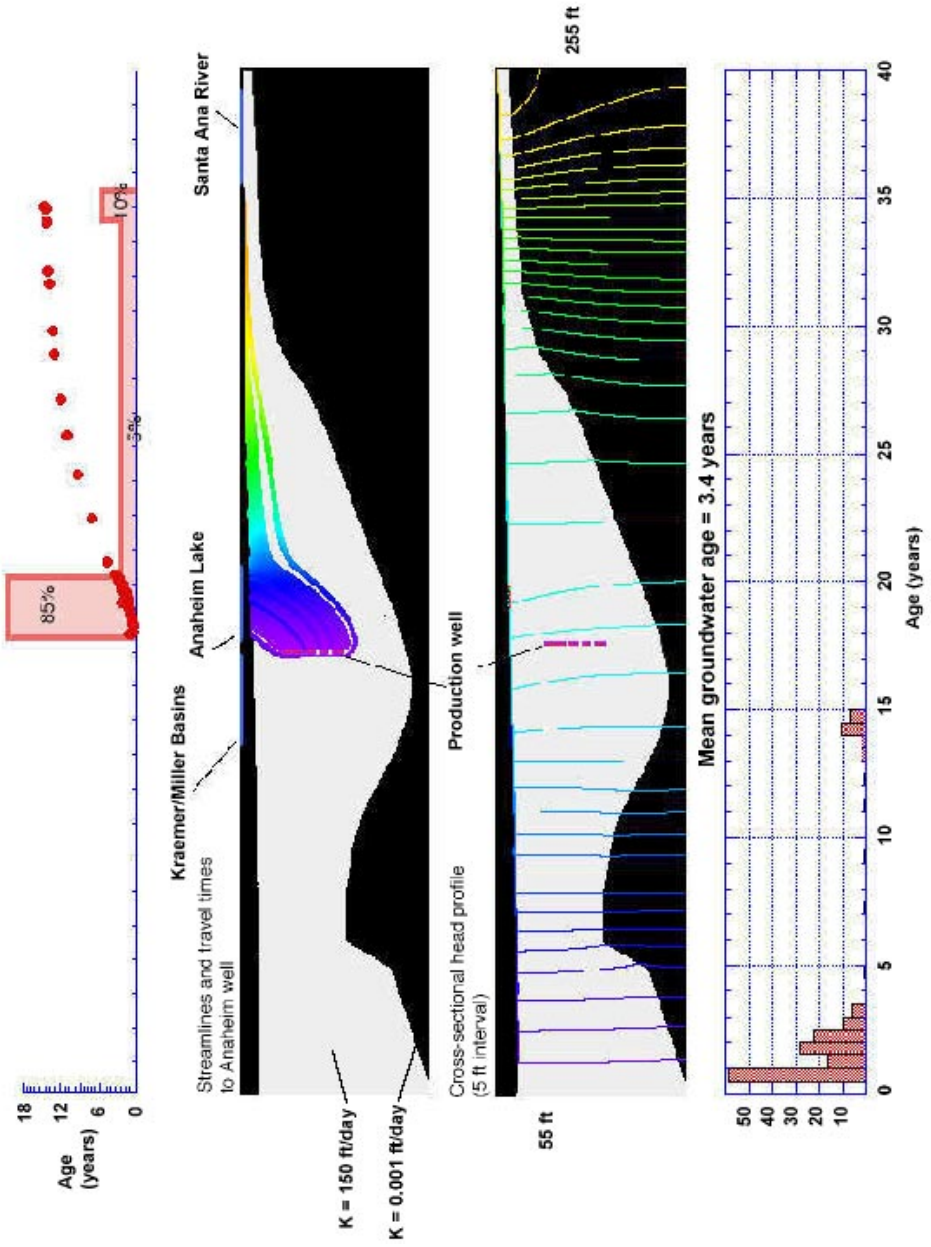
Age (years)
18
12
6
0
85%
10%
5%
Santa Ana River
Anaheim Lake
Kraemer/Miller Basins
Streamlines and travel times to Anaheim well
K = 150 ft/day
K = 0.001 ft/day
Production well
Cross-sectional head profile (5 ft interval)
255 ft
55 ft
Mean groundwater age = 3.4 years
50
40
30
20
10
0
5
10
15
20
25
30
35
40
Age (years)

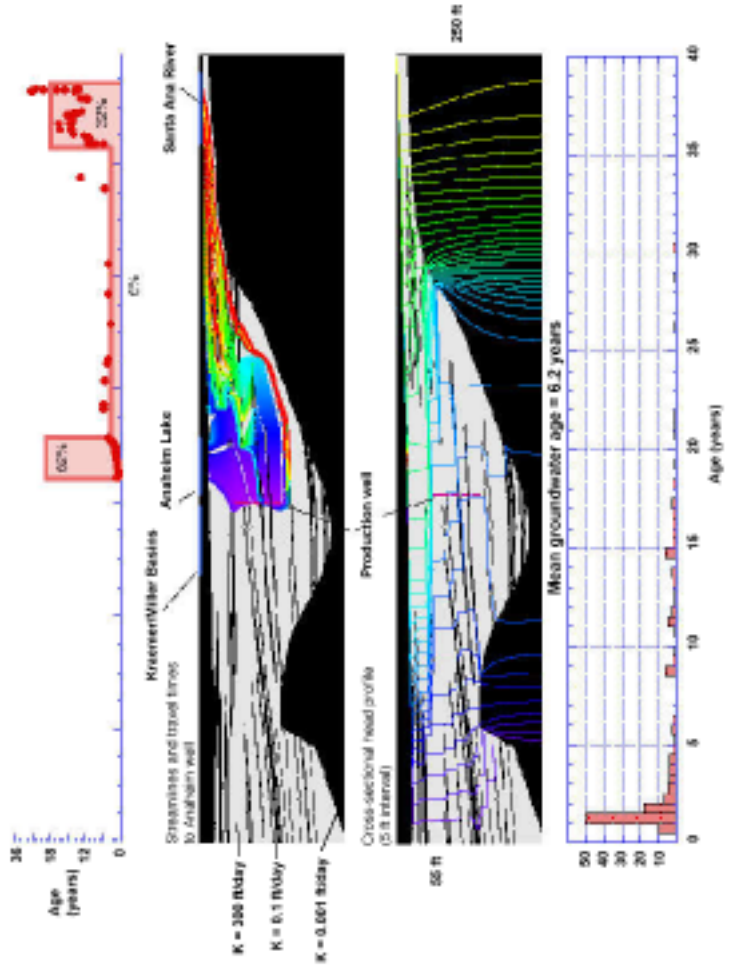

Figure 5: Results from two-dimensional scoping simulation in the Forebay cross-section. Cross-sectional images show hydraulic head contours and backward travel pathways from the "Anaheim" well to surface recharge points. Travel pathways are color-coded to represent time of flight. Vertical and horizontal dimensions of the section are 1,900 and 28,000 ft, respectively. Top figure represents spatial location and time of flight along streamlines connecting the well to surface recharge points. Shaded areas represent the fraction of water captured in the well coming from Anaheim Lake, natural rainfall to the east, and the Santa Ana River, respectively. Bottom figure represents the age distribution of water entering the well. Part (a) based upon conductivities of 200 ft/day and 1 ft/day in the permeable and semipermeable materials, respectively. Part (b) based upon a uniform conductivity of 150 ft/day in both the permeable and semipermeable materials. Part (c) based upon conductivities of 300 ft/day and 0.1 ft/day in the permeable and semipermeable materials, respectively.

river, and 3% from rainfall recharge. The model-determined age distribution ranges between 2 and 18 years and shows distributional peaks that correspond with the lake (young) and river (old) inputs. The model-determined mean age of 4.6 years (see Appendix) is much smaller than the 12-18 y isotopically determined age.

In Figure 5b, a uniform hydraulic conductivity of 150 ft/day was used throughout the domain, except for the basement. As a result, the hydraulic heads and streamlines vary much more smoothly. The fraction of lake water in the well has risen to 85%, while the fraction of river water has declined to 10%. The age of water entering the well ranges from 2 to 15 y. The model-determined mean age was reduced to 3.4 y.

In Figure 5c, the conductivity in the permeable materials was raised to 300 ft/day while that in the semipermeable zones was reduced correspondingly to 0.1 ft/day. As one would expect, the impacts of heterogeneity can be clearly seen in the head contours and streamline plots. Very strong breaks in the head occur across the semipermeable zones. Streamlines follow increasingly circuitous routes around corners and breaks in the zones. The resulting fraction of lake water in the well decreased to 62%, while the fraction of river water increased to 32%. Additionally, the age of water entering the well was spread over a larger range (2 to 30 y) with an increased model-determined mean of 6.2 y.

The two-dimensional simulations clearly indicate that the distribution of age (or residence time) of water in the well can span decades, even though the average simulated ages are much less than the isotopically-determined values. In addition, the simulations indicate that the source of water in the "Anaheim" well is clearly distributed, but typically dominated by the Anaheim Lake inputs.

Geologic heterogeneity clearly impacts the results. In comparing Figures 5, 5a, and 5c, we see that increasing heterogeneity in the conductivity distribution (*i.e.,* a greater spread in the extrema of the binary distribution) systematically

- Raises the average residence time of captured well water (model or reinterpreted age),
- Raises the span or variance of ages in the water, and
- Decreases the fraction of lake water appearing in the well with a corresponding increase of river water.

Although the two-dimensional simulations provide several useful insights, they are limited in their overall quantitative value. The first and foremost issue lies in their two-dimensionality. The two-dimensional setting literally forces river water to always appear in the well and exacerbates, to some extent, the complexity of flow pathways shown in Figure 5c. As long as river and lake water appear in the well, the rainfall recharge between the lake and river is *always* captured in the well. The extra degree of freedom in a three-dimensional world will allow streamline motion around 2D barriers and prevent the kind of hydraulic discontinuity shown in the head contours of Figure 5c. Potentially larger mean travel times, consistent with the

isotopic data, may become likely. The presence of river water in the "Anaheim" well would not be assured by the conceptual setup alone. And of course, the specification of well discharge and basin recharge could be made in a manner more consistent with actual field behavior.

4 Toward a more realistic three-dimensional model

We are now concerned with building a more realistic three-dimensional model of groundwater flow in the Forebay recharge area. As a result of the previous simulations, this model is based upon the observation that heterogeneity and three-dimensionality are important and need to be effectively represented to achieve more meaningful results.

Our flow model will again be based upon a direct representation of geologic heterogeneity. As a provisional modeling domain, we have selected a three-dimensional volume extending roughly 1,500 ft beneath the larger rectangular area shown in Figure 3. This area is roughly 29,000 ft (5.5 mi) long and 10,000 ft (1.9 mi) wide, and it is bounded by the Santa Ana River. The bottom of the domain is approximately 1,300 feet below sea level. The top corresponds roughly with the water table at the northwest side, which is about 100 ft beneath the ground surface. The orientation of the two-dimensional cross-section shown in Figures 4 and 5 inside of this area is shown in Figure 6.

4.1 Philosophy of geologic representation

In the absence of a three-dimensional analog of the cross-sectional interpretation shown in Figures 4 and 5, we have developed an independent geologic representation within the model volume using a transition probability/Markov geostatistical indicator technique (Carle, 1996; Carle, *et al.* 1998). This approach seeks to represent the spatial distribution and correlation of discrete, hydraulically-distinct geologic materials in such a way that borehole information is honored and inferred material length scales and architectural features are statistically reproduced throughout the domain. Multiple system "realizations" can be produced in this fashion, representing, in effect, different "interpretations" that are consistent with known borehole data and specified geologic architecture. Once material classes are identified and simulated, material properties are assigned and used to drive flow simulations, as was done earlier in the two-dimensional model.

This approach is grounded in the assumption that the geologic data provides the most detailed information on the heterogeneity of hydraulic properties throughout the aquifer system, and the spatial distribution of aquifer and aquitard materials is primarily related to geologic architecture. In particular, low-permeability materials are attributed to clays, silts, and siltstones, and high-permeability materials are attributed to sands, gravels, sandstones, and conglomerates. Presumably, the geologic architecture creates preferential flow paths and localized barriers that become the dominant cause of dispersion and mixing within the aquifer system.

This particular geostatistical technique is used as a practical means for instilling a plausible degree of geologic detail and realism, while honoring as much of the available geologic data as possible. It avoids several simplifying assumptions and operational limitations associated with Gaussian models of random permeability variability (Tompson, *et al.*, 1989), specifically the high-permeability bias inherent

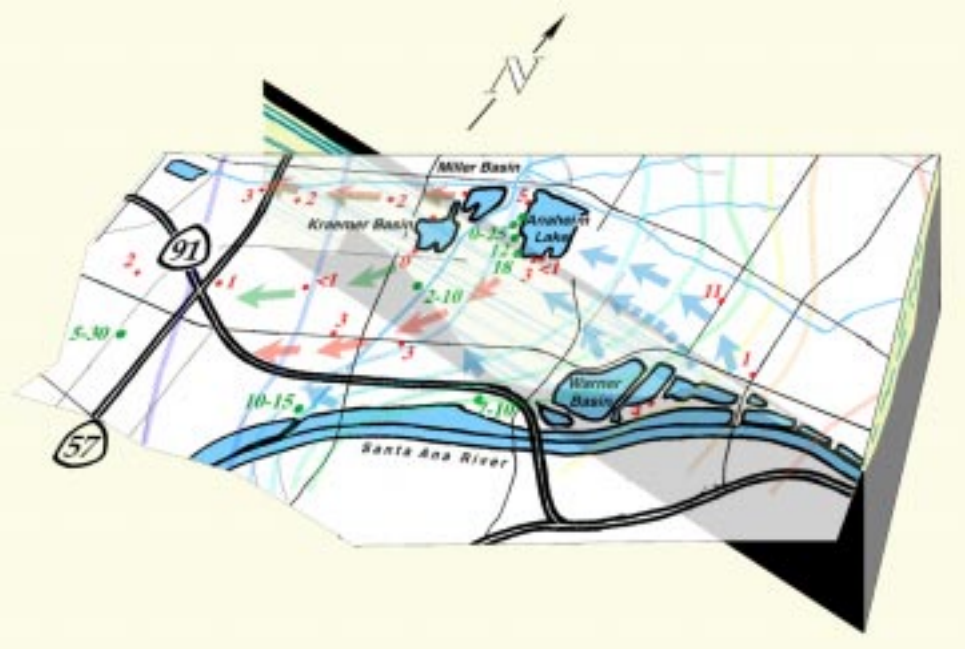

Figure 6: Three-dimensional conceptual view of the Forebay area showing the orientation of the cross section used in Figs. 4 and 5. Solid wide arrows show shallow groundwater flow paths inferred from isotopic analyses. Dashed wide arrows show deeper flow paths. The color of the arrows represents the inferred source of water, with blue representing Santa Ana River recharge, red representing Anaheim Lake recharge, and green representing Kraemer/Miller basin recharge. Approximate hydraulic head contours inferred from well data are also shown. Estimated groundwater ages made in samples from production or monitoring wells are also shown. Red numbers generally represent measurements from shallow wells screened at depths less than 500 ft, although the size of the sample (screen length) is not indicated. Green numbers represent measurements from wells with screens extending beyond 500 ft in depth. A range of numbers generally represents a range ages determined from a multilevel monitoring well with small sampling intervals.

in typical permeability data sets used to construct them, as well as a decreased ability to recreate or incorporate specific forms of geologic heterogeneity.

4.2 System geology

Geologic materials in the middle to lower portion of the model domain are composed of unconsolidated to semi-consolidated Quaternary sedimentary deposits that overlay consolidated Tertiary sedimentary (basement) rocks of low estimated permeability. Materials in the upper part of the domain are composed of Holocene and late Pleistocene alluvial deposits to 275 feet in thickness. Several Pleistocene sedimentary formations may underlie the surficial alluvium; however, an exacting subsurface mapping is not available. As a result, the geologic model development rests on geologic interpretation of the available information.

Data considered in development of the geologic model include driller's logs, a soils map, and geologic maps, reports, and cross-sections. The driller's logs consist of records of soil descriptions based mostly upon cuttings taken at irregular intervals. Driller's logs from 24 wells ranging in depth from 150 to 1,500 ft helped to identify dominant material textures and define the spatial scales of vertical variability (Fig. 3). Lateral spatial continuity of alluvial gravels, sands, and fines was inferred from a soils map (Wachtell, 1978) using an approach demonstrated by Weissmann *et al.* (1998). Several geologic cross-sections constructed by the Orange County Water District (OCWD, written communication) distinguish high- and low-permeability materials based upon geophysical and driller's logs. These cross sections indicate increasing folding with depth, but no displacement of beds as a result of faulting (except, possibly, near the lower portion of the domain at its western/southwestern boundary). Geologic maps and reports were used to identify the geologic formations that likely underlie the surficial alluvial deposits.

Our geologic model assumes that the Alluvial deposits unconformably overlie the La Habra (mid- to late-Pleistocene) and deeper San Pedro (early Pleistocene) Formations. The non-marine La Habra Formation chiefly consists of fluvial-derived sandstone, conglomerate, and siltstone materials. The San Pedro Formation consists of marine and non-marine sandstone, conglomerate, and siltstone materials and is underlain by the Tertiary basement rocks. Notably, the San Pedro Formation constitutes the most prolific water-bearing zone in the aquifer system. Within the model volume, the La Habra Formation and San Pedro Formation are likely folded and, possibly, vertically displaced by faulting. Although older hydrogeologic cross sections (California Department of Water Resources, 1967) have indicated buried fault-bounded horst structures, more recent hydrogeologic interpretations (OCWD, written communication) differ in the degree to which faulting is shown in this portion of the aquifer system.

4.3 Generation of the geologic representation

The geologic model domain was divided into 4 subvolumes based on the interpretation of the local geologic formations: *Qal* (alluvial deposits), *Qlh* (La Habra Formation), *Qsp* (San Pedro Formation), and *Tb* (Tertiary basement). The choice of material classes and specification of spatial variability was developed separately and independently in the upper three subvolumes, considering that each formation is bounded by unconformities. *Tb* was assumed homogeneous. The complete geologic model was constructed by patching each of the subvolumes together in stratigraphic order. Folding was specified within the *Qlh* and *Qsp* subvolumes at this stage. Formation thickness estimates (California Division of Water Resources, 1967; Yerke, 1972) and recent OCWD cross-sections guided the demarcation of upper and lower contacts of the formations, as well as their degree of folding.

The Alluvial, LaHabra, and San Pedro subvolumes (*Qal*, *Qlh*, and *Qsp*) were each divided into three hydrologic categories, as shown in Table 1. To develop the geostatistical models of spatial variability, estimates of the followings parameters were required (Carle and Fogg, 1997):

- Volumetric proportions (p) of each category,
- Mean widths ($\overline{w}$), lengths ($\overline{l}$), and thicknesses ($\overline{t}$) with respect to the principal stratigraphic directions (strike, dip, and vertical) for each category, and
- Conditional probabilities that one category occurs adjacent to the other (the juxtapositional tendencies).

The principal stratigraphic directions in each sublayer were ultimately chosen to conform with gross folding patterns. Before accounting for folding, the strike direction in each subvolume was assumed horizontal and parallel with the longer side (y-axis) of the domain, the dip direction was assumed horizontal and parallel with the short side (x-axis) of the domain, and the vertical direction was truly vertical (z-axis). Folding was implemented by applying slight rotations in the dip direction throughout various parts of the *Qlh* and *Qsp* subvolumes.

Reasonable estimates of the class proportions could be inferred from driller's logs, geologic cross sections, and geologic descriptions. The parameter $\overline{t}$ was estimated from driller's logs (for *Qal)*, a measured section (for *Qlh*; Yerke, 1972), and geologic cross-sections (for *Qsp).* The parameters $\overline{w}$ and $\overline{l}$ were inferred from the soils map for the alluvial deposits and estimated from geologic cross-sections for the other formations. For simplicity, and because of a lack of data, the juxtapositional tendencies were assumed statistically independent (random), which can be calculated according to the assumed proportions and the $\overline{w}$, $\overline{l}$, and $\overline{t}$ parameters associated with each category (Carle and Fogg, 1997). The full set of parameters obtained is shown in Table 1. These parameters were used to prescribe a 3-D Markov chain model of spatial variability (Carle and Fogg, 1997) and implement a geostatistical

Table 1: Categorical abundance (p) and length ($\overline{w}$, $\overline{l}$, and $\overline{t}$) parameters used in the geostatistical model of Alluvial, La Habra, and San Pedro formations.

Category	p	$\overline{w}$ (ft)	$\overline{l}$ (ft)	$\overline{t}$ (ft)
Qal gravel	0.35	250	800	3.5
Qal sand	0.53	350	1000	5
Qal fines	0.12	300	667	1.9
Qlh conglomerate	0.25	350	1000	9
Qlh sandstone	0.45	800	2000	15
Qlh siltstone	0.25	1000	2000	20
Qsp conglomerate	0.25	2000	2000	20
Qsp sandstone	0.45	3000	3000	50
Qsp siltstone	0.30	4000	4000	40
Tb	1.0	-	-	-

conditional simulation algorithm for each subvolume, as based on successive application of sequential indicator simulation (Deutsch and Journel, 1992) and simulated quenching (Aarts and Korst, 1989; Carle, 1997; Carle *et al.*, 1998).

Figure 7 shows a three-dimensional perspective of a single realization of geologic architecture in the model volume obtained after the individual subvolume realizations are recombined. In order to properly resolve spatial variability, the categorical data were simulated on a uniform, orthogonal grid with a discretization equal to 100 ft along the y-axis (original strike direction), 50 ft along the x-axis (dip direction) and 2 ft along the z-axis (vertical direction). The model volume realized in the figure contains over *45 million* nodal points (or blocks).

4.4 Flow model approach

Because of computer access and other time limitations, a subsection of the geologic model shown in Figure 7 was initially used to develop a steady groundwater flow simulation. The smaller flow domain is 17,500 ft (3.3 miles) long and 7,500 ft (1.4 mi) wide, as shown in Figure 3. The thickness was also reduced to 1,382 ft by removing the bottom 100 ft of the of the original domain. The Santa Ana River was assumed to bound the entire upper, southeast side of the smaller domain. The resolution of the geologic architecture was preserved in the flow model and resulted in a problem with over *18 million* blocks. Scalar values of hydraulic conductivity

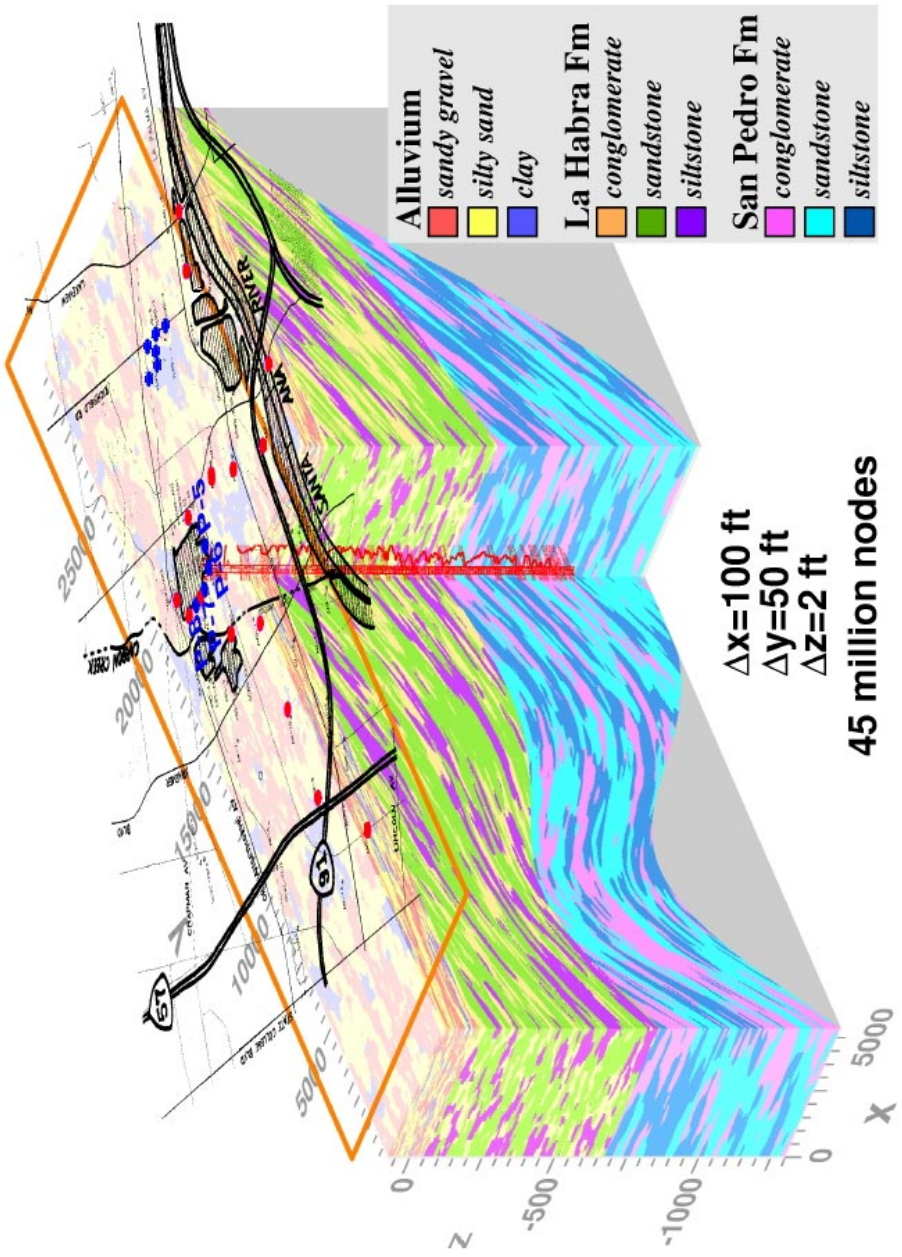

Figure 7: Three-dimensional geologic realization of the modeling domain lying beneath the large rectangular area shown in Figure 3. The smaller modeling domain discussed in the text was extracted from this realization.

were assigned to the material classes and adjusted within the calibration process.

Flow simulations were based upon a standard 7-point stencil finite volume method implemented within the ParFlow computer model (Ashby, 1996; Tompson *et al.*, 1998). This model is designed to readily solve large, steady flow problems on parallel or scalar platforms and is based upon an efficient and scaleable multigrid preconditioned conjugate gradient algorithm (Ashby and Falgout, 1996). These simulations were performed on a 10-processor DEC Alphaserver 8400.

Flow results were determined with steady boundary conditions and did not account for transients in the recharge, pumping, or underflow specifications. Along the northeast (upgradient) side of the domain, an underflow flux of 500,000 ft^3/day was allowed to enter the *Qal* and *Qlh* subvolumes, with no flux crossing into the *Tb* subvolume. This was estimated from a regional, two-dimensional model developed by OCWD (personal communication). Along the northwest vertical face, an outward underflow flux was allowed to leave the *Qal* and *Qlh* subvolumes, and its magnitude was adjusted as part of the calibration process. Along the southwest (downgradient) face of the domain, the hydraulic head was fixed at a hydrostatic value of 80 ft above sea level. No-flow conditions were specified along the bottom and southeast vertical face of the domain.

Along the top of the domain, uniform fluxes through five recharge basins (Fig. 3) were specified in accordance with the average annual data shown in Table 2. These data were obtained by observing the recharge operations directly. The Santa Ana River value represents 2/3 of the actual observation; the remaining portion was assumed to recharge to the south of our domain. Rainfall recharge in the amount of 0.00027 ft/day (0.1 ft/yr) was also distributed through the top of the model. Steady pumping from 10 extraction wells was specified according to the data in Table 3. With this information, a simple mass balance shows the total flux exiting the domain through the northwest and southwest vertical boundaries must sum to approximately 1.32×10^7 ft^3/day.

The current flow simulations will be used to estimate the source and age distribution of groundwater in wells P5, P6, and P7 using the reverse streamline technique described earlier. Comparisons with the isotopic ages shown in Table 3 will be used as an aid in calibration, as well as to illustrate the complexity of flow in the system and its impacts on the apparent isotopic ages (see Appendix).

4.5 Calibration and specification of hydraulic conductivity

Hydraulic conductivity values were assigned to each material category based upon typical ranges for the given lithologies (Anderson and Woessner, 1992) and local measurements and observations made by OCWD. They were adjusted within a calibration process seeking to match observed heads, approximate groundwater travel times, and groundwater source locations. The categorization of material properties in each subvolume sought to distinguish lower permeability (aquitard) materials, whose conductivities are typically not characterized, from the majority of aquifer materials.

Table 2: Approximate average daily recharge specified in each basin, as determined from annual measured totals (OCWD, personal communication). Santa Ana River System flux represents 2/3 of the total observed value, with the remaining portion assumed not to recharge the model volume.

Location	**Recharge** (ft^3/day)
Santa Ana River System	7,130,000
Kraemer Basin	3,274,000
Anaheim Lake	2,456,000
Warner Basin	1,404,000
Miller Basin	978,000

Well test data and previous two-dimensional modeling studies have indicated that the highest hydraulic conductivities in the Forebay range from 200 to 800 ft/day. Gross estimates of conductivities in the alluvium based upon isotopic travel time data and consideration of the fluvial depositional environment have been as large as 3,000 ft/day (M. L. Davisson, personal communication). Gravels and sands in *Qal* were generally assigned rather large conductivities, reflective of this information, while clays in the *Qal* were assigned much lower values. Considering that the San Pedro Formation has been described as a principal water bearing zone, hydraulic conductivities in *Qsp* were assumed greater than in *Qlh*, albeit much smaller than in *Qal*. Hydraulic conductivity of the low-permeability materials in each unit, including *Tb*, has not been investigated in detail, and so relatively small values were assigned and tested within the calibration process.

The calibration process strived to attain consistency with observed hydraulic heads. Throughout the process, it was found that several plausible sets of hydraulic conductivity values could be used to produce an approximate match to the observed hydraulic head distribution. Initially, the northwest end of the domain was considered to be a no flux boundary so that all subsurface flow exited the domain through the southwest boundary. In all of these cases, the simulated mean age of groundwater reaching well P6 was never greater than 6 y, certainly much smaller than the 17.7 year isotopically-measured age. In addition, many of the earlier simulations indicated that little, if any, groundwater in this well originated from the Santa Ana River, as has been suggested by the interpretations of Davisson *et al.* (1996) (Fig. 6).

As a result, two steps were taken to improve the simulations. In the first, the conductivity of the low permeability materials was reduced in order to impede near-vertical flow of younger water (from Anaheim Lake and Miller and Kraemer Basins)

Table 3: Pumping rates specified in production wells in the 3D flow model. Screen elevations are with respect to sea level (OCWD, personal communication). Isotopic ages determined by helium-tritium analyses of Davisson *et al.* (1996); some additional ages observed in monitoring wells are shown in Fig. 3. These wells are shown as blue dots in Figs. 3 and 7.

Well	**Screen elevation** $\mathbf{z}_{bottom}$(ft)	$\mathbf{z}_{top}$(ft)	**Screen length** (ft)	**Pumping rate** (ft^3/day)	**Isotopic age** (yrs)
P4	-56	34	90	207,393	-
P5	-128	-16	112	210,353	2.8
P6	-948	-198	750	548,653	17.7
P7	-976	-296	680	315,994	11.7
P8	-896	-216	680	674,058	-
PL1	-87	163	250	51,558	-
P1	-87	163	250	51,492	11.4
PL2	-78	92	170	84,768	-
PL3	-90	116	206	140,232	-
PL4	-156	161	317	298,045	-
PL5	-250	169	419	28,390	-

and to accentuate lateral flow from the Santa Ana River toward well P6. To maintain consistency with observed heads, conductivities were also adjusted upwards in the high permeability zones, as had been done in the earlier two-dimensional simulations. Although this step served to induce flows from the river to well P6, as had been observed, it was not possible to significantly raise the simulated mean ages beyond 6 y without producing inconsistently high head distributions. Nevertheless, it did confirm that the permeability of the aquitard materials has a real and significant impact on the flow field, despite the typical perception that these materials and their properties are unimportant or inconsequential. This was also been observed in multiwell transient pump test analyses of Carle (1996).

Hence, the second step involved specification of a nonzero flux out of the domain along its northwest boundary, essentially as a fraction or percentage of the total underflow known to exit the domain. This allowed lower conductivities to be specified in *Qlh* and *Qsp*, slowing the rates of travel, while still permitting reasonable matches in the hydraulic head distribution. In hindsight, outflows along this boundary seem quite reasonable in terms of the observed head contours shown in Figure 6.

Table 4 shows the hydraulic conductivities used in five most recent flow simulations, along with the percentage of underflow specified to exit the northwest

Table 4: Hydraulic conductivities assigned to the geologic categories in six "calibrated" flow simulations labeled *y* through *c*. Northwest flux represents percentage of total outward flux (excluding well pumping) specified along the northwest boundary of the domain.

Category	**Hydraulic conductivity**, K (ft/d)				
	y	*z*	*a*	*b*	*c*
Qal gravel	1000	1000	1000	1000	1000
Qal sand	200	200	200	200	200
Qal fines	1	1	1	1	1
Qlh conglomerate	2	4	5	6	8
Qlh sandstone	10	30	25	30	40
Qlh siltstone	0.1	0.1	0.1	0.1	0.2
Qsp conglomerate	10	10	15	20	20
Qsp sandstone	50	50	75	100	100
Qsp siltstone	0.1	0.1	0.1	0.1	0.2
Tb	0.1	0.1	0.1	0.1	0.1
Fractional underflow past northwest boundary (%)	50	45	40	35	30

boundary of the domain. These results and the subsequent travel time estimates will be discussed further below.

4.6 Results and observations

Figure 8 shows a three-dimensional perspective of the hydraulic head distribution obtained from flow simulation *c*. Significant "mounds" in the head distribution are associated with recharge from the Santa Ana River/Warner and the Anaheim Lake/Kraemer/Miller basins. The model generally agrees with the conceptualization of Figure 6 that shows flow originating from Santa Ana River area moving toward the northwest and wrapping around toward the west-southwest. Importantly, the model demonstrates the three-dimensionality of the flow system. The dipping geologic structure causes a downward component to preferential flow along high-permeability conduits. The heterogeneity creates a clear "stairstepping" of the head contours,

with strong downward gradients (or breaks) across zones of low permeability.

Streamlines connecting the screened interval of well P6 to upgradient recharge boundaries were constructed in all flow simulations, in a manner similar to that used in the two-dimensional scoping model and by Schafer-Perini *et al.* (1991). Ten streamlines were launched from a circular pattern in each grid block housing a pumping well element in the model. The flux entering the well in each block was evenly assigned to each streamline for determining mean groundwater ages, as discussed in the Appendix.

Figure 9 shows three-dimensional streamline trajectories from flow simulation *c*, color-coded to indicate backward time-of-flight. The flow paths are preferentially connected through well-defined channels in the aquifer system. Water entering the upper 20% or so of the well screen clearly originates from recharge in Anaheim Lake. This water travels along near-vertical flow paths and is generally less that 8 years old. Water entering the deeper portions of the well generally comes from the Santa Ana River and Warner recharge basins. This water is typically greater that 10 years old, with increasingly older water at greater depths in the well. The flow paths are more circuitous as they move around low permeability barriers. The fact that their initial trajectories are strongly confined within the high permeability alluvial materials is consistent with previous conceptualizations about shallow, high velocity recharge pathways (see also Fig. 6).

A histogram of travel time along the 4,000+ streamlines considered in this simulation is shown in Figure 10. The age distribution of water entering the well ranges nonuniformly from 2 to 52 y, with no water less that 1 y in age. Peaks in the distribution correspond to different source locations, the earliest (< 8 y) being the Anaheim Lake and Kraemer/Miller basins, the two intermediate peaks (8 to 20 y) being the Warner basin and closer portions of the Santa Ana River, and the latter (> 20 y) being the more distant part of the Santa Ana River.

When weighted by the flux in each streamline, the *true mean age* of the P6 well water is 16.0 y (see Appendix), which is somewhat less than the 17.7 isotopically measured age. As noted in the Appendix, the isotopically measured age is more closely approximated by an *apparent mean age* dependent on the historical levels of ^{3}H input into the groundwater. If the historical inputs are assumed constant, the simulated apparent age is a smaller 15.3 y; if the model input of Figure 13 is used, the simulated apparent age increases to 16.7 y, closer to the isotope measurement. These results are tabulated in Table 5, along with similar measurements made in four previous flow simulations that were calibrated (only) to the head observations. Here it is easy to see how the adjustments in conductivity values and the fractional underflow released through the northwest boundary (Table 4) combine to influence the mean ages of water reaching P6; runs *b* and *c* seem to be the best calibrated in terms of both head and mean age.

In Figure 11, streamline trajectories between well P7 and upgradient recharge areas are shown in the same fashion as before, again for flow simulation *c*. Here we see more indirect flow paths, possibly affected by diversions around the capture zone of P6 or other realization-dependent aspects of the geologic architecture. As

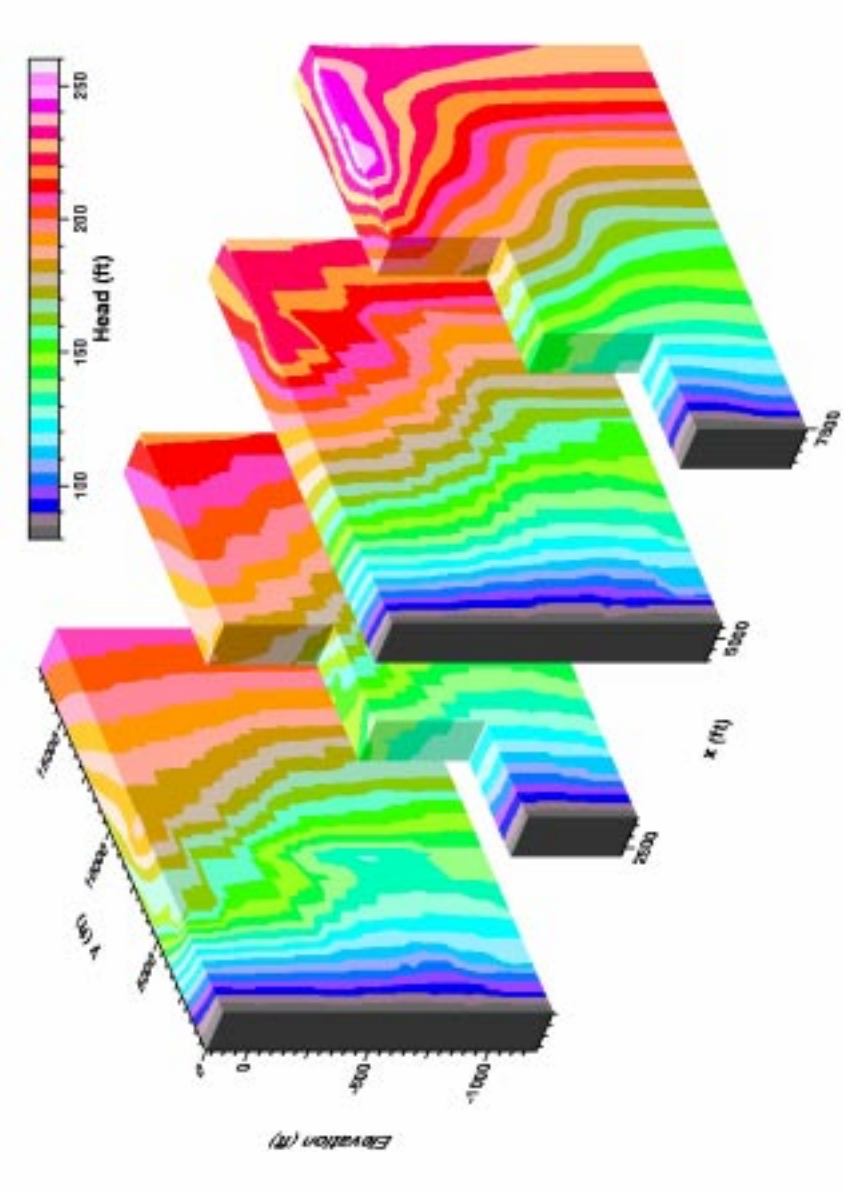

Figure 8: Three-dimensional perspective view of the modeled hydraulic head field from simulation *c*.

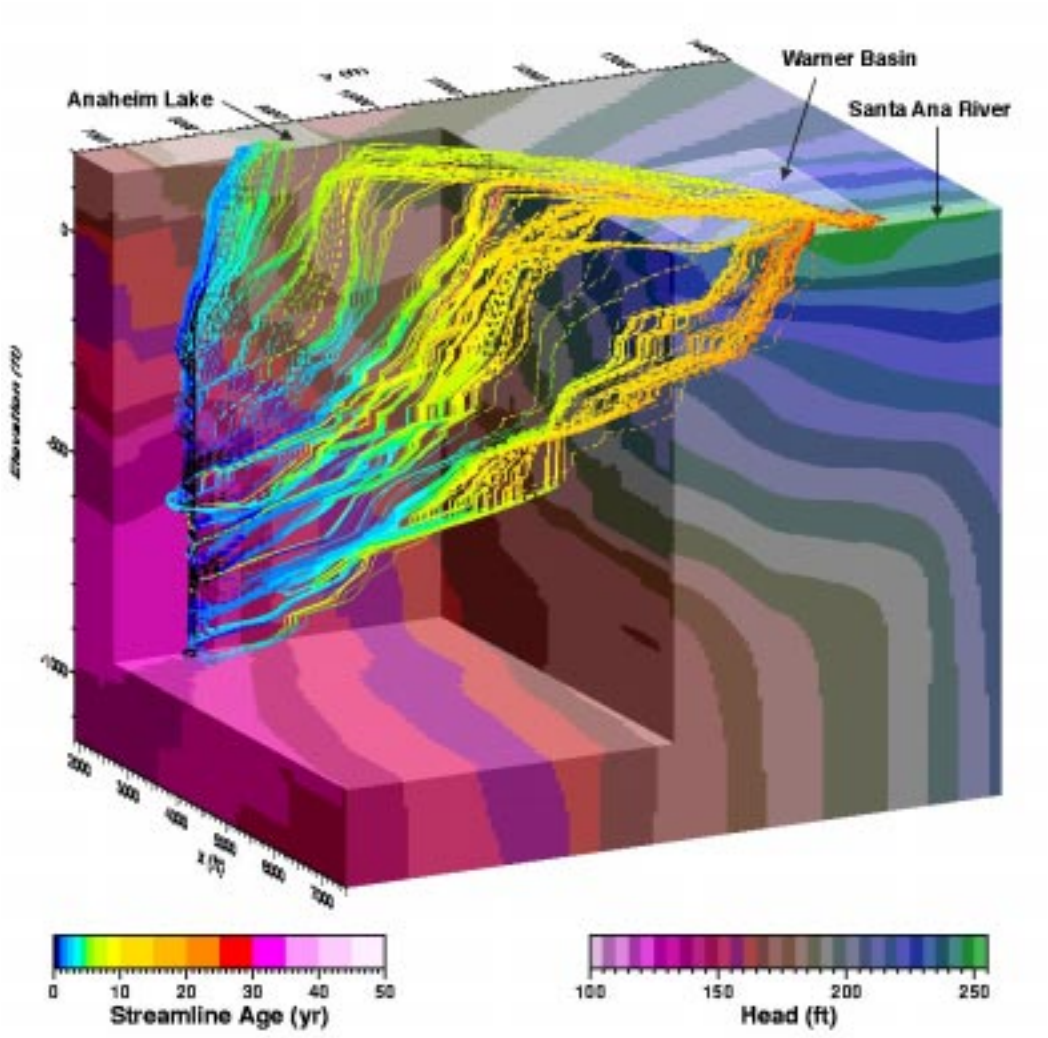

Figure 9: Close-up perspective of backward travel pathways from well P6 using flow simulation *c*. Streamlines are color-coded to indicate backward time-of-flight between the well and surface recharge points. Dashed lines indicate portions of streamlines "hidden" within background block, which is also color coded to indicate hydraulic head.

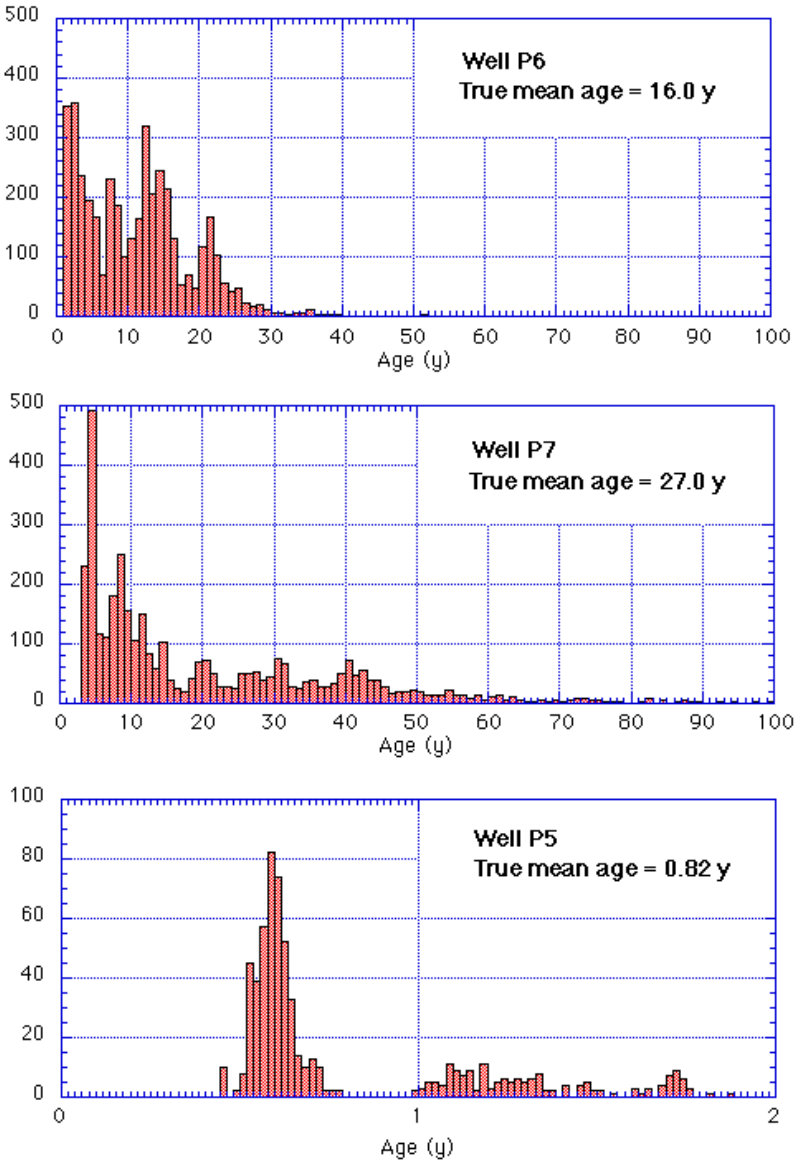

Figure 10: Distribution of model-predicted groundwater ages for wells P6, P7, and P5 based upon flow simulation *c*. One-year intervals shown for P6 and P7 histograms; one week intervals shown for P5 histogram.

Table 5: Simulated ages of groundwater at well P6 computed from calibrated flow simulations y, z, a, b, and c, where $\langle t \rangle$ is the modeled mean age, $\langle t \rangle_{A,EI}$ is an "apparent" age based upon a historically constant ^{3}H input, and $\langle t \rangle_A$ is the "apparent" age based upon the variable ^{3}H input shown in the Appendix. Simulated groundwater ages at wells P7 and P5 are also shown for flow simulation c.

	Well P6					**Well P7**	**Well P5**
Age (y)	y	z	a	b	c	c	c
$\langle t \rangle$	27.8	24.6	19.8	18.3	16.0	27.0	0.82
$\langle t \rangle_{A,EI}$	23.4	21.4	18.3	17.0	15.3	19.9	0.81
$\langle t \rangle_A$	28.3	25.3	20.6	19.0	16.7	28.5	0.84

in P6, the upper part of P7 captures water from Anaheim Lake, while the lower portion captures water from Warner basin and the Santa Ana River. The pathlines connected to the lower part of P7 are much more circuitous and involve relatively longer travel times. This is evident in the age distribution shown in Figure 10 which indicates travel times ranging from 4 to over 100 y. Although the younger portion of the P7 distribution is similar to that of well P6, the older parts are more widely distributed.

The *true mean age* of the P7 well water is 27.0 y (Appendix), much larger than the 11.7 y isotopically measured age. The simulated apparent age ranges between 19.9 and 28.5, depending on historical input of ^{3}H considered (Table 5). Not only do the large travel times associated with the right side of the distribution contribute to the large mean age, but higher streamline fluxes in the deeper locations do so as well. A closer inspection of the lower part of P7 showed a relatively long section of high permeability (as inferred from the well logs) which causes the larger simulated fluxes.

Interestingly, when the travel time data beyond 33 y in the histogram are ignored, the true mean age of the P7 well water is reduced to 11 y. Although the streamlines in this reduced distribution account for 2/3 of the total flow into the well, they are distributed over 3/4 of the well screen length. In other words, the older tail of the distribution carries a disproportionate (1/3) fraction of the flow, which is most likely focused on the bottom 1/4 of the well screen. Inspection of Figure 11 seems to confirm this.

Figure 12 shows the streamline trajectories for the smaller and shallower well, P5, as well as wells P6 and P7, all of which were based on flow simulation c. Water in P5 is completely and quickly derived from Anaheim Lake, as is shown by the true mean age of 0.82 y and essentially equivalent apparent ages of 0.81 and 0.84

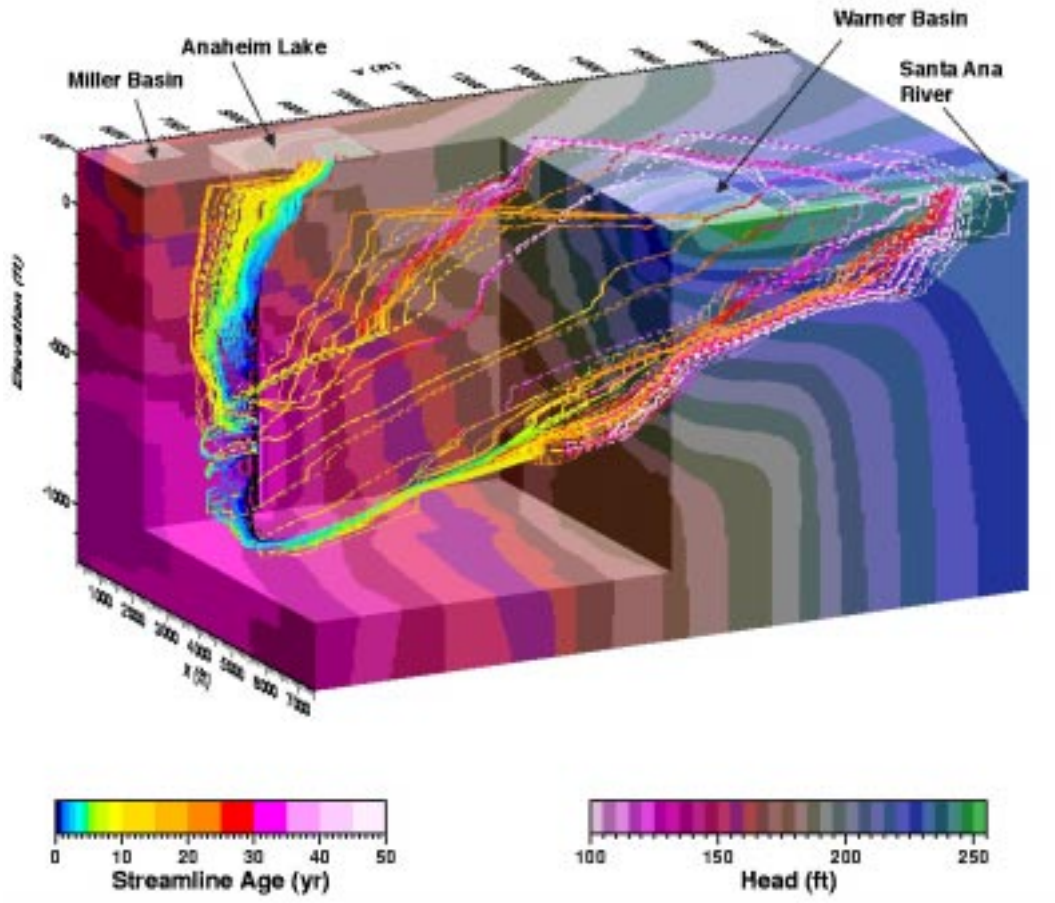

Figure 11: Close-up perspective of backward travel pathways from well P7 using flow simulation *c*. Streamlines are color-coded to indicate backward time-of-flight between the well and surface recharge points. Dashed lines indicate portions of streamlines "hidden" within background block, which is also color coded to indicate hydraulic head.

y (Table 5). These ages can be compared with the isotopically-determined value of 2.8 y. Although the age distribution of water reaching P5 spans 0 to 2 y, the detail in Figure 10 shows a bimodal structure, possibly related to two principal flow paths connecting the well to Anaheim lake. Most likely, this behavior is dependent on the particular geologic realization used and could easily differ if the well were moved slightly or a different realization were used.

Notably, the simulations suggest that very young water, less than a year old, is not apparent in wells P6 or P7, even though it is apparent in the shallower well P5. If the simulations are correct in this respect, then the proposed "residence" time requirements would be met for P6 and P7, but not for P5. A recent experiment involving the introduction of an Xe gas tracer into Anaheim Lake (Davisson, *et al.*, 1998) seems to be consistent with this behavior: the Xe tracer *was not* observed in wells P6 or P7 during the year following its introduction, even though it *was* observed in wells P5 and P8. Although P8 was not included in the current transport simulations, it is close to, and screened at similar depths as P6 and P7. Disproportionately large fluxes into the top of P8 have been inferred by Davisson, *et al.* (1998). These facts suggest that small scale variability in the geologic structure are contributing to these differences.

Although the apparent mean groundwater age simulated in well in P6 compares favorably with the isotopic age, the lack of agreement in the other wells is also indicative of the true variability in the geologic structure and flow complexity that develops in natural systems. Although many aspects of the discrepancies may be dependent on the realization or on the particular model of geologic architecture used (see below), others may be related the lack of transient effects in the simulations or upon overidealized geometry used to build the model domain and assign boundary conditions. Nevertheless, the simulations do reveal many of the complexities that occur as recharged groundwater makes its way to production wells – how the composition of well water can be highly mixed and its age distribution nonuniformly distributed. They also illustrate how isotopic data can be a powerful tool within the overall model calibration process.

4.7 On the issue of modeling and uncertainty

The geology beneath the percolation basins is well understood to be complex and heterogeneous. This is known from borehole geology, marked variabilities in flow paths and ages inferred from isotopic and simpler 2D modeling analyses, and general knowledge of flow behavior in clastic depositional systems. Heterogeneity will create complicated flow paths, occlude the interpretation of isotopic or other tracer data, and make understanding the system much more difficult. Although our modeling approach attempted to address this complexity, it is still uncertain in many respects.

The geologic model used (Fig. 7) represents a particular interpretation, or "realization" of the detailed geologic structure of the system created from analyses of borehole and other geologic data and an "automated" geostatistical algorithm. Although the accuracy of the realization (and the subsequent flow simulation) at any

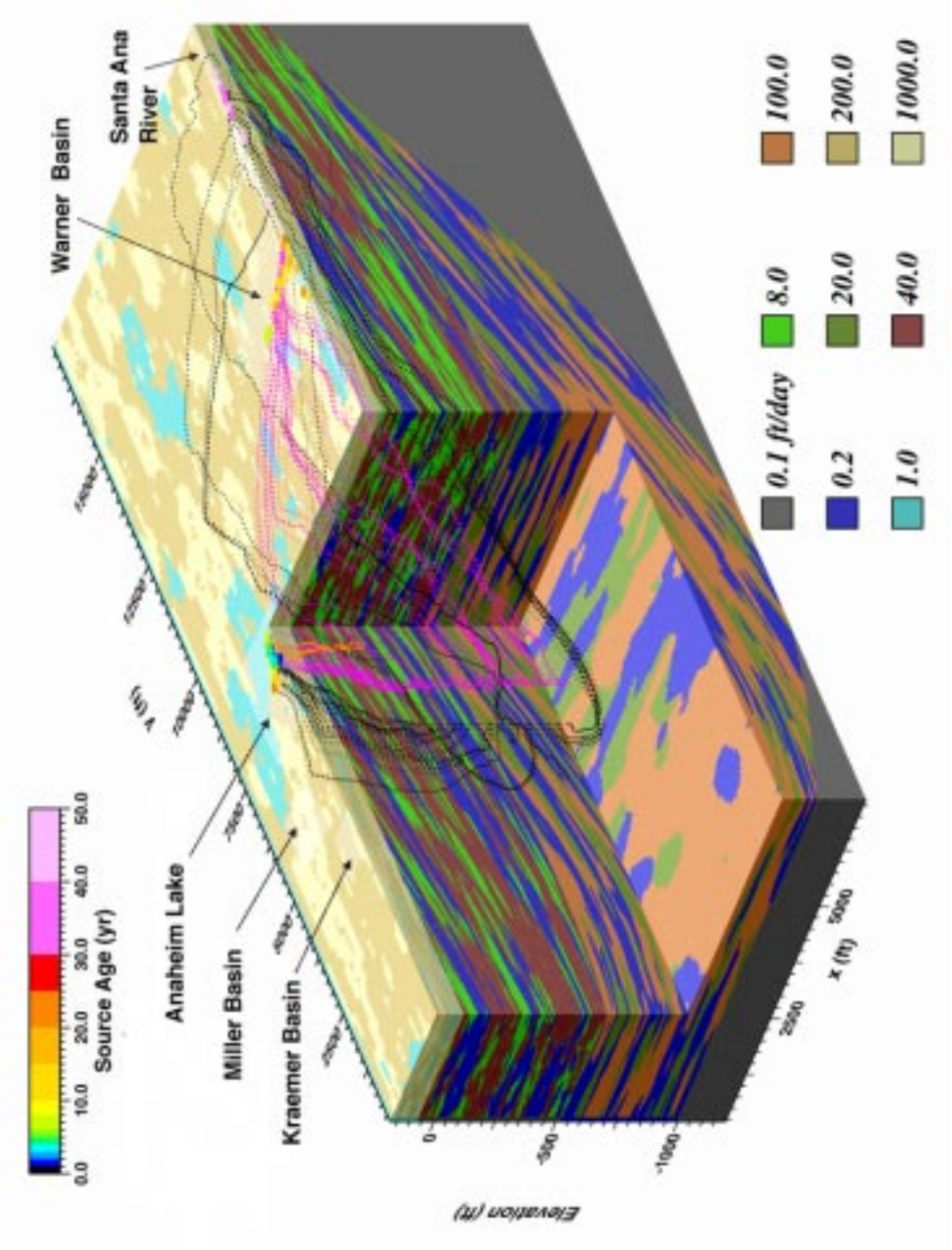

Figure 12: Complete perspective of selected backward travel pathways from wells P5, P6, and P7 using flow simulation *c*. Streamlines are color-coded to indicate the relevant capture well. Dashed lines indicate portions of streamlines "hidden" within background block, which is also color coded to indicate hydraulic conductivity. Dots represent intersection of streamlines with recharge surface and are color coded to travel time.

particular point may be uncertain, other equally-likely realizations and simulations are possible – just as many different cross-borehole interpretations may be provided by different geologists. Clearly, if our interpretation of the principal geologic materials, features, and length scales is accurate or plausible, then single or Monte Carlo simulations would clearly reflect a "representative" degree of behavioral complexity in the system and provide some insight into larger-scale "integrative" behavior (such as, for example, a proper estimate of the mean groundwater age and age distribution in a well). New insights are obtained through the process of model calibration, including consideration for geology, hydrology, and, particularly, isotopic age and source information.

It is more likely that modifications to the gross specifications in our geological model may be necessary, as a result of the provisional nature of these first simulations, or because the particular aspects of geologic realism embedded in the geostatistical algorithm are too simplified. This could lead to inaccuracies in the representative behavior observed in the model.

Nevertheless, coarser models that do not explicitly incorporate any degree of direct geologic complexity are subject to more severe limitations, largely because interpretations required to link (the same) geologic data and small-scale observables to model parameters and interpretation (as in traditional stochastic models; *e.g.,* Gelhar, 1993) may be too simplified or nonexistent. Thus, we believe that our detailed approach offers a logical and more satisfying way (albeit intensive) to analyze this system from a modeling perspective.

5 Conclusions and future directions

5.1 The feasibility aspect

Understanding the transport and fate of reclaimed water that is returned to the groundwater regime is needed to forecast long-term impacts on groundwater quality and to provide improved perspectives for the design of proper regulatory controls. A principal goal in this analysis was to demonstrate the *feasibility* of using a highly-resolved model to examine the complexity of groundwater flow and its influence on migration pathways and residence time distributions in the OCWD Forebay recharge system, as well as provide an alternative framework from which isotopic data and analyses could be interpreted.

The geology-based approach for describing heterogeneity is practical in the sense that the data required are standard and widely available (*e.g.,* geophysical or driller's logs, cross-borehole geologic interpretations, measured sections and cross-sections). The geostatistical approach automates the development of a geologic model of heterogeneity while accounting for a range of geologically plausible interpretations. Our intention was to demonstrate that, given some knowledge of the geology, whether from hard data or through geologic interpretation, geostatistics can be used to generate a geologically realistic model. Solution of multimillion-node flow systems is now becoming practical on modern computers. The streamline transport technique is computationally efficient and accurate. Thus, the package of the geostatistics and flow and transport modeling capabilities has made high-resolution modeling of complicated groundwater flow paths readily feasible.

5.2 A recap of insights

Several new insights related to the OCWD recharge system and use and interpretation of groundwater isotopic data have been obtained from this modeling study. These perspectives include:

- Detailed modeling has illustrated how the age of groundwater entering a production well can be highly distributed. The age distribution is affected by heterogeneity of the system and size of the sampling instrument (i.e., well screen). The fact the age is distributed may qualify how isotopic information can be used to demonstrate compliance with residence-time regulations or infer source, mixing and other variables related to water quality concerns.

- Because tritium-helium dating techniques are nonlinear with respect to mixing, the mean of the modeled age distribution in a mixed well sample should not necessarily be compared with an isotopic age based upon the same mixed sample. However, the model results can be reinterpreted in a way that is more consistent with the methods used in isotopic dating.

- Modeling has shown the composition of production well water may be derived from various sources. The distribution or sources and groundwater composi-

tion is affected by heterogeneity of the system. Current interpretations of the source of P6 well water in the OCWD system from the provisional model are consistent with gross interpretations inferred from isotopic analyses.

- Flow solutions were sensitive to conductivity values assigned to low permeability sediments. Relatively small values were required to induce significant lateral flow from the Santa Ana River towards the modeled production well and achieve consistency with isotopic interpretations. This again emphasizes importance of heterogeneity, and is in agreement with previous analyses in heterogeneous systems.

- The importance of heterogeneity reflects the importance of the geologic model and requisite resolution needed for a simulation. Although such a model can never be made complete, the current geology-based approach seems to offer a rational basis for incorporating existing or new data.

- Two dimensional models were unable to replicate realistic wells, flow pathways and travel times, largely because of their missing degree of freedom.

- Calibration of the model was greatly aided by the availability of the isotopic analyses. Mean age data allowed discrimination among equally-acceptable simulations calibrated to head data only. Improved understanding of the Orange County system has been obtained via a coordinated integration of isotopic analyses, advanced geologic modeling techniques, and a large-scale numerical simulation framework.

- The modeling exercise provided unique and invaluable insights toward understanding the complicated nature of the flow system. With continued calibration, the model should prove useful as a tool for prediction.

5.3 The future

Future work on the Forebay groundwater model might include a number of activities. Improved and more refined geologic models based upon additional borehole analyses, geologic interpretation, and parametric calibration could be made. A larger flow domain with a more careful analysis of the applied boundary conditions might remove potential boundary effects in the solution and lead to more credible estimates of the upgradient underflows. Forward and backward migration analyses could be used to analyze the composition of water in additional wells, as well as forecast the fate of specific waters released in specific basins. Analysis of multiple realizations would provide additional insight into uncertainties produced by the geostatistical approach. Incorporation of contaminant degradation models might be used to more thoroughly examine the role of decay and transformation. Incorporation of semi-temporal flow fields can be used to reflect the periodic nature of artificial recharge operations. Coordination with newer isotopic studies should also be continued.

6 Acknowledgments

This work was performed at Lawrence Livermore National Laboratory (LLNL) under contract W-7405-ENG-48 for the U. S. Department of Energy (DOE). We are deeply indebted to Doris Bruckner, Roy Herndon, John Reilly, Timothy Sovich, and Greg Woodside of the Orange County Water District in Fountain Valley, CA and to Steve Ashby, Chuck Baldwin, Bill Bosl, Lee Davisson, Rob Falgout, Bryant Hudson, and Steven Smith of LLNL for their collaboration and interest in this project.

7 Appendix

Groundwater samples extracted for age dating purposes may be mixed with respect to tritium and helium abundance if the sampling volumes are large. This may occur with a production-type well or if there is a significant level of aquifer dispersion. When tritium-helium age-dating methods are employed, use of mixed samples may lead to an *apparent mean age* that is different from the *true mean age* of the sample because isotopic dating is nonlinear with respect to mixing (Schlosser, 1992).

Here, we review a procedure to evaluate the model results in terms of the sampling methods employed in the field, so as to produce a reinterpreted age from the model that can be compared with the isotopically-determined apparent age.

7.1 Numerical evaluation of the true mean age

Consider the motion of a small fluid "packet" along a steady groundwater flow streamline that intersects the water table and enters the groundwater at time 0. Let $X(t)$ denote the molar tritium (^{3}H) concentration in this fluid packet, where $X^0 = X(0)$. Clearly, in the absence of small-scale diffusion or dispersion processes,

$$X(t) = X^0 e^{-\lambda t}, \tag{1}$$

where the decay rate λ is related to the 12.3 y half-life by $\lambda = \ln 2/t_{1/2}$. Let $Y(t)$ denote the molar helium-3 concentration (^{3}He) produced by radioactive tritium decay in the packet. Assuming that this decay mechanism is the only source of helium-3, then

$$Y(t) = X^0 - X(t) = X^0(1 - e^{-\lambda t}), \tag{2}$$

and the age or residence time of this packet may be determined by

$$t = \frac{1}{\lambda} \ln \left(1 + \frac{Y(t)}{X(t)} \right). \tag{3}$$

This does not require knowledge of the initial tritium loading, X^0, and is the key result behind the tritium-helium dating technique.

Now consider a family of N streamlines that connect a pumping well with the water table in an otherwise steady groundwater flow system, such as those shown in Figure 5. It is assumed that each streamline i corresponds to the center of an associated streamtube (*e.g.,* Thiele *et al.*, 1996) through which the fluid flux, Q_i, is fixed, and that the total flux in all streamtubes intersecting the well is equal to the total well pumping rate, $Q_w = \sum_{i=1,N} Q_i$. These are essentially the same streamlines calculated in the two- and three-dimensional simulations discussed above. Fluid packets moving along each streamline can be associated with a travel time t_i between the well and the water table. The mean age of groundwater entering the well may then be estimated in terms of the arithmetic mean over all streamlines, as weighted by the individual fluxes, *e.g.,*

$$\langle t \rangle = \frac{\sum_{i=1,N} Q_i t_i}{\sum_{i=1,N} Q_i} = \frac{1}{\lambda} \sum_{i=1}^{N} \frac{Q_i}{Q_w} \ln \left(1 + \frac{Y_i(t)}{X_i(t)} \right) \tag{4}$$

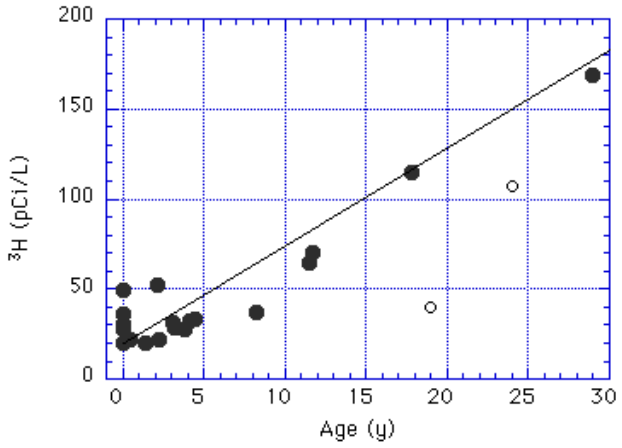

Figure 13: Estimates of historical tritium input concentration into groundwater in the Forebay, prior to 1995, as inferred from Figure 12 of Davisson *et al.* (1996). Open circles denote data affected by evaporation that were not used in a linear fit (G. Hudson, personal communication, 1998).

This is a numerical estimate of the *true mean age* of the well water.

7.2 Numerical evaluation of the apparent mean age

The *apparent mean age* is determined from a ratio of the total helium and total tritium found in a well sample. As such, it is subject to a mixing effect produced by extracting water from the entire screened interval of the well, and may differ from the result in (4). In terms of the N streamlines used in the flow simulations, it can be estimated from

$$\langle t \rangle_A = \frac{1}{\lambda} \ln \left(1 + \frac{\langle Y_i \rangle}{\langle X_i \rangle} \right) = \frac{1}{\lambda} \ln \left(\frac{\sum_{i=1,N} Q_i X_i^0}{\sum_{i=1,N} Q_i X_i^0 e^{-\lambda t_i}} \right). \tag{5}$$

Numerical evaluation of the *apparent mean age* will require information on the initial tritium loading, or value of X_i^0, along each model streamline, in addition to the streamline travel times and fluxes. It is generally reasonable to expect the historical tritium input to increase significantly over the past few decades as a result of bomb-pulse tritium releases (*e.g.,* Davisson *et al.*, 1996). Although this can be difficult to measure, and may be subject to some degree of error, Davisson *et al.* (1996) have attempted to estimate the input in the Forebay area, as shown in their data that is reproduced in Figure 13. A simple fit to the more reliable data indicates

$$X_i^0 = X^0(t_i) \approx 20 + 5.4 t_i, \tag{6}$$

whence $\langle t \rangle_A$ can be estimated from the numerical results.

If the historical tritium inputs were all equal, $\langle t \rangle_A$ would become independent of X^0 and (5) would reduce to

$$\langle t \rangle_{A,EI} = \frac{1}{\lambda} \ln \left(\frac{Q_w}{\sum_{i=1,N} Q_i e^{-\lambda t_i}} \right). \tag{7}$$

7.3 Implications

From a numerical calibration or validation perspective, $\langle t \rangle_A$ is the most appropriate type of mean to compute for comparison with isotopically-determined values from the field. It is, nevertheless, sensitive to the shape and form of the input function (*e.g.,* eq.6) used. Under most circumstances, the apparent age under equal-input conditions will be less than both the true mean and the apparent age under historically rising tritium inputs (as reflected in Figure 13), *e.g.,*

$$\langle t \rangle_{A,EI} < \langle t \rangle \tag{8}$$

$$\langle t \rangle_{A,EI} < \langle t \rangle_A. \tag{9}$$

Although problem-specific considerations will govern how $\langle t \rangle_A$ compares with $\langle t \rangle$, these inequalities are evident in the simulations summarized in Table 5.

Simulated values of $\langle t \rangle$ and $\langle t \rangle_A$ obtained from (4) and (5) will be sensitive to resolution of the model and the number of streamlines used to resolve variation of flow patterns into the well. Interestingly, in the limit as $N \rightarrow 1$ (low model resolution) or as the well screen length $\rightarrow 0$ (small measurement scale), the two measures will converge such that $\langle t \rangle_A \approx \langle t \rangle$ (see results for well P5 in Table 5). This suggests that better measurements of the true mean age or the vertical distribution of ages over a vertical segment in a well might be best obtained from a multi-level monitoring scheme with small individual sampling scales at each measurement location.

References

[1] Aarts, E., and Korst, J. (1989), Simulated annealing and Boltzmann machines: John Wiley & Sons, New York, 272 p.

[2] Anderson, M. P. and W. W. Woessner (1992), Applied groundwater modeling : Simulation of flow and advective transport Academic Press, San Diego

[3] Ashby, S. F. and R. D. Falgout (1996), A parallel multigrid preconditioned conjugate gradient algorithm for groundwater flow simulations, Nuclear Science and Engineering, 124(1), 145-159.

[4] Ashby, S. F. (1996): ParFlow home page: http://www.llnl.gov/CASC/ParFlow/

[5] California Department of Water Resources (1967), Progress report on ground water geology of the coastal plain of Orange County, California Department of Water Resources, Sacramento

[6] Carle, S. F. (1996), A Transition probability-based approach to geostatistical characterization of hydrostratigraphic architecture: Ph. D. dissertation, University of California, Davis, 238 p.

[7] Carle, S. F. (1997), Implementation schemes for avoiding artifact discontinuities in simulated annealing: Mathematical Geology, v. 29, p. 231-244.

[8] Carle, S. F., and Fogg, G. E. (1997), Modeling spatial variability with one- and multidimensional Markov chains: Mathematical Geology, v. 28, p. 453-476.

[9] Carle, S. F., Labolle, E. M., Weissmann, G. S., Van Brocklin, D., and Fogg, G. E. (1998), Conditional simulation of hydrofacies architecture: a transition probability/Markov approach: *in* Hydrogeologic Models of Sedimenary Aquifers, Concepts in Hydrogeology and Environmental Geology No. 1, G. S. Fraser and J. M. Davis, eds., Society for Sedimentary Geology, Tulsa, OK, 147–170.

[10] Celia, M. A. and W. G. Gray (1992), Numerical Methods for Differential Equations, Fundamental Concepts for Scientific and Engineering Applications, Prentice Hall, Englewood Cliffs, NJ, 436p.

[11] Davisson, M. L., G. B. Hudson, R. Herndon, S. Niemeyer and J. Beiriger (1996), Report on the feasibility of using isotopes to source and age-date groundwater in Orange County Water District's Forebay Region, Orange County, California, Lawrence Livermore National Laboratory, UCRL-ID-123593

[12] Davisson, M. L., G. B. Hudson, J. B. Moran, S. Niemeyer, and R. Herndon (1998), Isotope tracer approaches for characterizing artificial recharge and demonstrating regulatory compliance, proceedings, Annual UC Water Reuse Conference, Monterey, CA, June 4-5, 1998.

[13] Deutsch, C. V., and Journel, A. G. (1992), Geostatistical Software Library and User's Guide: Oxford University Press, New York, 340 p.

[14] Gelhar, L. W. (1993), Stochastic Subsurface Hydrology, Prentice Hall, 390 p.

[15] Goode, D. J. (1996), Direct simulation of groundwater age, Water Resources Research, 32(2), 289-296

[16] Hudson, G. B., M. L. Davisson, C. A. Velsko, S. Niemeyer, B. K. Esser, and J. Beiriger (1995), Preliminary report on isotope abundance measurements in groundwater samples from the Talbert Injection Barrier Area, Orange County Water District, Lawrence Livermore National Laboratory, UCRL-ID-122450

[17] Nir, A. (1954), On the interpretation of tritium "age" measurement in groundwater, Journal of Geophysical Research, 69, 2589

[18] OCWD (1991), Groundwater Management Plan, 1991 Update, Orange County Water District, Fountain Valley, CA

[19] OCWD (1995), Orange County Water District Annual Report, 1994-1995, Orange County Water District, Fountain Valley, CA

[20] Schafer-Perini, A. L., J. L. Wilson, and M. L. Perini (1991), Efficient and accurate front tracking for two dimensional groundwater flow models Water Resources Research, 27, 1471–1487.

[21] Schlosser, P. (1992), Tritium/^{3}He dating of waters in natural systems, in Isotopes of Noble Gases as Tracers in Environmental Studies, proceedings of a consultants meeting on isotopes of noble gases as tracers in environmental studies (Vienna, Austria, May 29 - June 2, 1989), 123-145, International Atomic Energy Agency, Vienna

[22] Thiele, M. R., R. P. Batycky, M. J. Blunt, and F. M. Orr (1996), Simulating flow in heterogeneous systems using streamtubes and streamlines, SPR Reservoir Engineering, February, 5–12

[23] Tompson, A. F. B., R. Ababou, and L. W. Gelhar (1989), Implementation of the three-dimensional turning bands random field generator, Water Resources Research, 25(10), 2227-2243.

[24] Tompson, A. F. B., R. D. Falgout, S. G. Smith, W. J. Bosl, and S. F. Ashby (1998), Analysis of subsurface contaminant migration and remediation using high performance computing, in press, Advances in Water Resources (also, http://www-ep.es.llnl.gov/www-ep/esd/sstrans/tompson/AWR96/).

[25] Wachtell, J. K. (1978), Soil survey of Orange County and western part of Riverside County, California: United States Department of Agriculture.

[26] Weissmann, G. S., Carle, S. F., VanBrocklin, D, and Fogg, G. E. (1998), Three-dimensional hydrofacies modeling based on soil survey analysis and transition probability statistics: Hydrogeology, *in press*.

[27] Williams, A. E. and D. P. Rodoni (1997), Regional isotope effects and application to hydrologic investigations in southwestern California, Water Resources Research, 33(7), 1721-1729.

[28] Yerkes, R. F. (1972), Geology and oil resources of the eastern Puente Hills, southern California: in Geology of the eastern Los Angeles Basin, U.S. Geological Survey Professional Paper 420-C, U.S. Geological Survey, Washington DC